Nanoscale

Accepted Manuscript

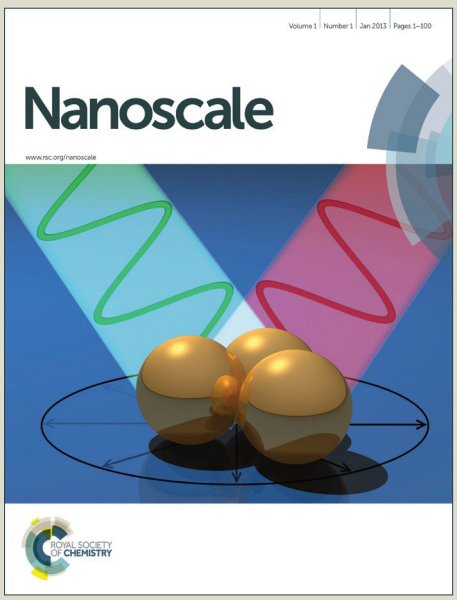

ROYAL SOCIETY OF CHEMISTRY

www.rsc.org/nanoscale

High-Performance, Flexible and Robust Metal Nanotrough-Embedded Transparent Conducting Film for Wearable Touch Screen Panels

Hyeon-Gyun Im,[a]† *Byeong Wan An,*[b]† *Jungho Jin,*[c] *Junho Jang,*[a] *Young-Geun Park,*[b] *Jang-Ung Park*[b]* *and Byeong-Soo Bae*[a]*

[a]Department of Materials Science & Engineering (MSE), Korea Advanced Institute of Science & Technology (KAIST), Daejeon, KOREA

[b]School of Materials Science and Engineering, Wearable Electronics Research Group, Center for Smart Sensor Systems, Ulsan National Institute of Science and Technology (UNIST), Ulsan Metropolitan City, 689-798, Republic of Korea

[c]School of Materials Science & Engineering (MSE), University of Ulsan, Ulsan Metropolitan City, KOREA

†These authors contributed equally to this work

Abstract

We report a high-performance, flexible and robust metal nanotrough-embedded transparent conducting hybrid film (metal nanotrough-GFRHybrimer). Using electro-spun polymer nanofiber web as a template and vacuum-deposited gold as a conductor, a junction resistance-free continuous metal nanotrough network is formed. Subsequently, the metal nanotrough is embedded in the surface of a glass-fabric reinforced composite substrate (GFRHybrimer). The monolithic composite structure of our transparent conducting film allows simultaneously high thermal stability (24 hr at 250 ^{o}C air condition), a smooth surface topography (R_{rms} < 1 nm) and an excellent opto-electrical property. A flexible touch screen panel (TSP) is fabricated using the transparent conducting films. The flexible TSP device stably operates on the back of a human hand and on a wristband.

Introduction

Transparent conducting electrode (TCE) with excellent mechanical flexibility will be salient components of next generation wearable optoelectronic devices such as light emitting devices, photovoltaic cells, switching devices, and touch screen panels.[1-4] Undoubtedly, tin-doped indium oxide (ITO) has been the most widely-used TCE material in both academic and industrial settings due to its optical transparency, thermal/chemical stability, device compatibility, and well-developed fabrication process.[5, 6] Despite the brittle nature of ITO, a large variety of wearable optoelectronic devices –of limited flexibility– have been fabricated on ITO TCE/plastic films.[7] Generally, the ITO's thickness is over 150 nm to ensure high conductivity. However, this thickness is not suitable for wearable optoelectronic applications due to ITO's small critical bending strain (ε_{crit}); for example, 150 nm of ITO mounted on a plastic film with thickness of 100 μm exhibits an ε_{crit} of 1.5 % upon bending radius of only 3.3 mm.[8, 9] In addition, the fluctuating cost of elemental indium also makes this material problematic for use in future optoelectronics.[10] It is not a simple task to prepare TCEs with high conductivity and high mechanical flexibility using ITO.

Potential alternatives to ITO include carbon nanotube (CNT), graphene, conducting polymers, metal nanowires (NW), metal meshes, and metal nanotrough networks.[11-22] Though carbon-based TCE materials such as CNT, graphene, and conducting polymers profoundly outperform ITO in terms of flexibility, their intrinsic low conductivity limits their viable use. On the other hand, metal-based TCEs such as metal NW, metal meshes, and metal nanotrough networks exhibit outstanding opto-electrical performance–for example, sheet resistance less than 10 Ω sq^{-1} at 90 % transmittance– as well as superior flexibility.[17, 23-25] In particular, a percolating network of one-dimensional (1D) metal nanotroughs is one of the most promising TCE materials due to its exceptional opto-electrical performance; a continuous and random network of metal nanotroughs allows high conductivity and Moiré pattern-free characteristics.[26] In addition, the excellent flexibility of the metal nanotrough network (ε_{crit} > 50 %) makes this material well-suited to wearable optoelectronic applications.[17]

On the other hand, metal nanotrough TCEs also have inevitable drawbacks, including: (1) weak adhesion to the substrate, (2) rough surface topography, and (3) poor thermal stability. Metal

nanotrough TCE must remain tightly mounted on the substrate to avoid delamination of the metal nanotrough TCE from the substrate. Also, the surface roughness of metal nanotrough TCE, which stems from the half-pipe shape of the metal nanotrough network, is one of the most critical sources of device malfunction and thus should be minimized. Finally, the thermal stability of metal nanotrough TCE should be guaranteed because the fabrication process for typical optoelectronic devices involves high-temperature annealing steps.

From the above considerations, we herein report a high-performance metal nanotrough-embedded TCE/film platform (hereafter, metal nanotrough-GFRHybrimer film). The metal nanotrough-GFRHybrimer film consists of a surface-embedded metal nanotrough network as a TCE and a glass fabric-reinforced composite plastic (GFRHybrimer) film[27] as a substrate. A surface-embedded and continuous network of metal nanotrough TCE allows excellent opto-electrical performance (sheet resistance of 4 Ω sq^{-1} at transmittance of 94 %), extremely smooth surface topography (the root-mean-square of the height variation (R_{rms}) < 1 nm, peak-to-peak value < 8 nm), and strong adhesion. The metal nanotrough-GFRHybrimer film also exhibits outstanding thermal robustness (24 h at 250 °C in air atmosphere) and superior inner/outer bending durability (10^4-cycles at bending radius of 1 mm). To demonstrate the potential suitability of the metal nanotrough-GFRHybrimer film as a flexible TCE platform, a wearable touch screen panel (TSP) was fabricated using the film. The TSP device exhibits stable operation on the back of a human hand and on a wristband.

Results and discussion

A schematic illustration of the fabrication process of the metal nanotrough-GFRHybrimer film is provided in Figure 1a. Briefly, a continuous water-soluble polymer nanofiber web is formed using electro-spinning process (Figure S1a), and then the polymer nanofiber web is annealed to weld individual fibers which can reduce height variation at junctions (Figure S1b, c). Average diameter of

the individual polymer fiber is 1 μm. Subsequently, metal is deposited on the polymer nanofiber web to build a continuous metal nanotrough network. The surface coverage area of the metal nanotrough network is controlled by the electro-spinning time of the polymer nanofiber web. After dissolving the polymer nanofiber web, the metal nanotrough network on a donor glass (Figure S2) is directly transferred onto a matrix resin-impregnated glass fabric sheet; the donor glass is surface-treated with octadecyltrichlorosilane to induce the release of the metal nanotrough network in the subsequent transfer process. The freestanding metal nanotrough-GFRHybrimer film is then peeled off after UV-curing of the matrix resin (Figure 1b). The detailed fabrication method is summarized in the Experimental Section. The embedded TCE structure of the metal nanotrough-GFRHybrimer film facilitates a tight encapsulation of the metal nanotrough TCE with minimal exposure for electrical contact as depicted in the scanning electron microscopy (SEM) images (Figure 1c and 1d). In addition, because most parts of the metal nanotrough is embedded in the matrix resin, an extremely smooth surface was achieved, as revealed by atomic force microscopy (AFM) analysis (Figure 1e). The R_{rms} of the metal nanotrough-GFRHybrimer film is less than 1 nm; the peak-to-peak line-scan value is less than 8 nm (white dotted line).

Typical metal nanotrough TCEs, due to their junction resistance-free continuous TCE structure,

exhibit opto-electrical performance superior to that of other percolatively nanostructured TCE materials such as metal NWs.[28] To evaluate the opto-electrical performance of the metal nanotrough-GFRHybrimer film, total optical transmittance at 550 nm (T_{tot}) with varying sheet resistance (R_{sh}) values is measured using a UV-vis spectrometer under GFRHybrimer base-line setting. The optical transmittance spectra of the films under the ambient air base-line setting are shown in Figure S3. The opto-electrical performance of the metal nanotrough-GFRHybrimer films can be controlled by varying the electro-spinning time of the polymer nanofiber web. A longer electrospinning time results in a denser network of the metal nanotroughs, thereby reducing the R_{sh} of the metal nanotrough-GFRHybrimer film. Transmittance decreases as the electrospinning time increases due to the

increased surface coverage of the metal nanotroughs (Figure S4). The electrical uniformity of the metal nanotrough-GFRHybrimer films can also be affected by the surface coverage area of the metal nanotroughs. As increasing electro-spinning time, the metal nanotrough-GFRHybrimer films exhibit better electrical uniformity (Figure S4a). Figure 2 shows a plot of T_{tot} versus R_{sh} for the metal nanotrough-GFRHybrimer films; reference data from recent, state-of-the-art TCEs are included for comparison.[29-33] The metal nanotrough-GFRHybrimer films exhibit excellent opto-electrical performance; for example, they show a value of R_{sh} = 4 Ω sq^{-1} with T_{tot} = 94 %. It is worth noting that the opto-electrical performance of the metal nanotrough-GFRHybrimer films is comparable to or even better than those of metal networks, AgNW networks, and CuNW networks that have been reported in the literature. The excellent opto-electrical performance of the metal nanotrough-GFRHybrimer film can be attributed to the continuous and junction-free characteristic of the metal nanotrough network.[17]

For a conventional TCE film, the opto-electrical performance can be expressed using a figure of merit defined by the Haacke equation.[34]

$$\Phi_{TC} = \frac{T^{10}}{R_{sh}} \quad (1)$$

where Φ_{TC} is the figure of merit, and T is the optical transmittance. The higher the Φ_{TC} value, the better the opto-electrical performance of a TCE will be. From Figure 2, the maximum and the average Φ_{TC} values of the metal nanotrough-GFRHybrimer films can be seen to be 174 x 10^{-3} Ω^{-1} (T: 90 %, R_{sh}: 2 Ω sq^{-1}) and 112 x 10^{-3} Ω^{-1}, respectively. For comparison, the Φ_{TC} values for typical TCEs such as those of crystalline-ITO, AgNW, and CuNW are also summarized in Table 1.[5, 18, 35] The metal nanotrough-GFRHybrimer films exhibit higher Φ_{TC} values than those of the reference TCEs. With this exceptional opto-electrical performance, the metal nanotrough-GFRHybirmer film can be suitable for high-performance optoelectronic device applications.

The thermal stability of a TCE is of great importance because most optoelectronic device fabrication processes involve high temperature annealing.[36, 37] Typical metal nanotrough TCEs exhibit weak thermal stability at high temperature condition.[26] To evaluate the thermal stability, the metal

nanotrough-GFRHybrimer film and the metal nanotrough on glass reference sample were oven-annealed at 250 ^{o}C under ambient condition; the R_{sh} values of the samples were collected during annealing. Figure 3a shows changes of the R_{sh} of the samples. It is noteworthy that changes of the R_{sh} of the reference metal nanotrough on the glass sample surged more than 500-times after 2 hr annealing. In sharp contrast, the metal nanotrough-GFRHybrimer film retained its initial electrical property even after 24 hr of annealing. Surface SEM images of the two samples also reveal the thermal stability of the samples (Figure 3b, 3c). After 24 hr annealing, disconnection of the nanotrough TCE is observed for the reference metal nanotrough on glass (Figure 3c inset). However, the metal nanotrough-GFRHybrimer film remains in its initial shape without any sign of disconnection or meltdown (Figure 3b). Temperature dependence of the metal nanotrough-GFRHybrimer film was also tested, in which a metal nanotrough-GFRHybrimer film was annealed up to 500 ^{o}C with a ramp rate of 5 ^{o}C min^{-1} (Figure S5). The R_{sh} of the metal nanotrough-GFRHybrimer film retained up to 440 ^{o}C and then rapidly increased which is likely due to the decomposition of the matrix.[19] The excellent thermal stability of the metal nanotrough-GFRHybrimer film can be attributed to the surface-embedded nanotrough network, which is optimally encapsulated by the thermal-insulating matrix while providing minimal surface opening of the nanotrough for electrical contact.

The mechanical robustness, including the bending durability and the adhesion stability of the TCE, should be guaranteed because performance degradation of devices under external mechanical stress mostly stems from the failure of the TCE layer, which shows a dramatic increase in R_{sh}. To confirm the mechanical stability of the metal nanotrough-GFRHybrimer film, a series of mechanical tests were performed. A bending test for the metal nanotrough-GFRHybrimer film (60 μm), with varying of the bending radius, was conducted (Figure 3d). Commercial ITO/PET (150 nm of ITO on 200 μm of PET) was also tested for comparison. The metal nanotrough-GFRHybrimer films show unchanged R_{sh} values when bending radius reached 1 mm during both inner and outer bending tests. In contrast, the commercial ITO/PET sample started to crack at bending radius of 5.5 mm, showing 10-times increase of R_{sh}. Cyclic bending durability was also evaluated (Figure 3e). R_{sh} values of the metal nanotrough-GFRHybrimer films were measured under repeated bending tests (bending radius

was 1 mm). The metal nanotrough-GFRHybrimer film tolerated 10^4 inner/outer bending cycles and retained its initial resistance. In contrast, the R_{sh} values of the ITO deposited on the PET sample catastrophically increased 500-times after 10 cycles of bending (Figure S6). The outstanding flexibility of the metal nanotrough-GFRHybrimer film is a promising feature, making this material suitable for use in flexible optoelectronics.

The adhesion stability of the metal nanotrough-GFRHybrimer film was also evaluated using the 3M tape test (Figure S7). The metal nanotrough-GFRHybrimer film endured 100-cycles of the tape test, retaining its initial R_{sh} value. On the other hand, the reference metal nanotrough on the glass sample delaminated from the glass at once, losing its electrical conductivity. This strong adhesion property of the metal nanotrough-GFRHybrimer film, which originates from the surface-embedded TCE structure, will make this material useful for optoelectronic device applications.

To demonstrate the potential suitability of the metal nanotrough-GFRHybrimer film for flexible optoelectronic applications, a wearable touch screen panel (TSP, 4-wire resistive type) was fabricated using the metal nanotrough-GFRHybrimer films (Figure 4). Figure 4a provides schematic and photographic images of the fabricated TSP device. Both top and bottom electrodes were composed of the metal nanotrough-GFRHybrimer films; commercial photoresist (SU8) was used as the spacer. The fabricated TSP device was integrated on the back of a human hand (Figure 4b, S8). As can be seen in Figure 4d, the TSP device on the back of the human hand shows stable operation; it was possible to write the characters “KAIST”. The TSP device was also integrated on a wristband, and this structure also exhibited stable operation; it was possible to write the characters “UNIST” (Figure 4c, S9). Based on these results, our metal nanotrough-GFRHybrimer film can be seen as a promising TCE/film platform for flexible optoelectronic applications.

Conclusion

In summary, we have fabricated a high performance and robust TCE/film (metal nanotrough-

GFRHybrimer film) using a continuous metal nanotrough network as a TCE and a glass fabric-reinforced composite plastic (GFRHybrimer) film as a substrate. The continuous and junction-free metal nanotrough TCE is embedded on the surface of a GFRHybrimer film, providing minimal opening for electrical contact. The metal nanotrough-GFRHybrimer film exhibits excellent opto-electrical performance (R_{sh} = 4 Ω sq^{-1} with T_{tot} = 94 %) compared to those of recent state-of-the-art TCEs; it also has extremely smooth surface topography (R_{rms} < 1 nm, peak-to-peak value < 8 nm), superior thermal stability (24 hr at 250 ^{o}C air condition), and outstanding bending durability (10^{4}-cycles with bending radius of 1 mm). To demonstrate the potential of this metal nanotrough-GFRHybrimer film as a flexible optoelectronic device platform, a wearable touch screen panel (TSP) was fabricated. The TSP device was integrated on the back of a human hand and on a wristband; stable operation was confirmed. We believe that our metal nanotrough-GFRHybrimer film can be a promising candidate for the replacement of ITO and metal NW TCEs in optoelectronic applications.

Experimental

Fabrication of metal nanotrough

a polymer fiber web (template for metal nanotrough) was produced using electrospinning, a common method for making ultra-long polymer fibers at low cost and in large quantity. Polyvinylpyrrolidone (PVP, Aldrich), a water-soluble polymer, was selected as the electrospinning-polymer material. PVP powder was added to methanol (Aldrich) and stirred at room temperature for 1h to prepare the precursor solution (14 wt%). To produce the polymer fiber web, voltage of 9.2 KV was applied to the nozzle using a high-voltage applier (NanoNC), while the precursor solution was being sprayed. Subsequently, the free-standing polymer fiber web was collected in an aluminum frame (diameter of the frame is 4 inch). The free-standing polymer fiber web in the Al frame was then annealed at 150 ^{o}C for 1 h to induce welding of individual fibers; this welding process can reduce the height differences at junctions of the fibers. The density of the polymer fiber web was controlled according to the time. After drying, gold was deposited (100 nm) on the polymer fiber web using thermal evaporation. The

deposited gold nanotrough network was placed on the glass and washed with water to eliminate the polymer fiber web. Finally, a metal nanotrough network on glass was obtained after drying.

Fabrication of metal nanotrough-GFRHybrimer film

The pre-formed metal nanotrough network on glass was brought into contact with a glass fabric that had been impregnated with a thermally insulating matrix resin; resulting material was compressed. The matrix is a UV-curable transparent siloxane resin blend consisting of cycloaliphatic epoxy oligosiloxanes (CAEO) and bis-[1-ethyl(3-oxetanyl)]methyl ether (DOX) as a functional cross-linker.[38] Using a vacuum-bag molding process and UV-curing, the metal nanotrough-GFRHybrimer film was fabricated.

Characterization

The sheet resistance (R_{sh}) was measured using a 4-point probe sheet resistance meter; the measured R_{sh} values were also cross-checked using a multimeter. SEM images were obtained using a scanning electron microscope (s4800, HITACHI). An AFM image was obtained using a scanning probe microscope (XE-100, Park Systems). The bending tests were performed using a lab-made bending test tool.

Fabrication of touch screen panel

Commercial photo-resist SU8 3050 (MicroChem Corp.) was spin-coated (3000 rpm, 50 μm thickness) on a metal nanotrough-GFRHybrimer film (bottom TCE film) and then patterned using the photo-lithography process to form a dotted-spacer (diameter = 100 μm and distance between spacers = 1 mm). Using silver paste, two electrical outlets were produced on the bottom of the TCE film. Another metal nanotrough-GFRHybrimer film (top TCE film), which also had two electrical outlets, was brought into the contact with and bonded to bottom TCE film using a commercial adhesive (8265S, J-B weld). Finally, the films were connected to the TSP operation circuit (RS232, NTREX) *via* 4 copper wires.

Acknowledgement

This work was supported by the National Research Foundation of Korea(NRF) grant funded by the Korea government (MSIP) (CAFDC 5-3,NRF-2007-0056090), and this research was also supported by Basic Science Research Program through the National Research Foundation of Korea (NRF) funded by the Ministry of Science, ICT &Future Planning (2013R1A2A2A01068542).

Notes and references

1. W. Gaynor, S. Hofmann, M. G. Christoforo, C. Sachse, S. Mehra, A. Salleo, M. D. McGehee, M. C. Gather, B. Lussem, L. Muller-Meskamp, P. Peumans and K. Leo, *Adv. Mater.*, 2013, **25**, 4006-4013.
2. W. Gaynor, G. F. Burkhard, M. D. McGehee and P. Peumans, *Adv. Mater.*, 2011, **23**, 2905-2910.
3. M. S. Lee, K. Lee, S. Y. Kim, H. Lee, J. Park, K. H. Choi, H. K. Kim, D. G. Kim, D. Y. Lee, S. Nam and J. U. Park, *Nano Lett.*, 2013, **13**, 2814-2821.
4. J. Lee, P. Lee, H. B. Lee, S. Hong, I. Lee, J. Yeo, S. S. Lee, T. S. Kim, D. Lee and S. H. Ko, *Adv. Funct. Mater.*, 2013, **23**, 4171-4176.
5. S.-B. Kang, H.-J. Kim, Y.-J. Noh, S.-I. Na and H.-K. Kim, *Nano Energy*, 2015, **11**, 179-188.
6. Z. Chen, W. Li, R. Li, Y. Zhang, G. Xu and H. Cheng, *Langmuir : the ACS journal of surfaces and colloids*, 2013, **29**, 13836-13842.
7. B. J. Kim, D. H. Kim, Y.-Y. Lee, H.-W. Shin, G. S. Han, J. S. Hong, K. Mahmood, T. K. Ahn, Y.-C. Joo, K. S. Hong, N.-G. Park, S. Lee and H. S. Jung, *Energy Environ. Sci.*, 2015, **8**, 916-921.
8. Y. Leterrier, L. Médico, F. Demarco, J. A. E. Månson, U. Betz, M. F. Escolà, M. Kharrazi Olsson and F. Atamny, *Thin Solid Films*, 2004, **460**, 156-166.
9. O. Tuna, Y. Selamet, G. Aygun and L. Ozyuzer, *J. Phys. D: Appl. Phys.*, 2010, **43**, 055402.
10. *Journal*, 2015.
11. X. Wang, Z. Li, W. Xu, S. A. Kulkarni, S. K. Batabyal, S. Zhang, A. Cao and L. H. Wong, *Nano Energy*, 2015, **11**, 728-735.
12. H. Park and J. Kong, *Adv. Energy Mater.*, 2014, **4**, 1301280.
13. M. S. White, M. Kaltenbrunner, E. D. Głowacki, K. Gutnichenko, G. Kettlgruber, I. Graz, S. Aazou, C. Ulbricht, D. A. M. Egbe, M. C. Miron, Z. Major, M. C. Scharber, T. Sekitani, T. Someya, S. Bauer and N. S. Sariciftci, *Nat. Photon.*, 2013, **7**, 811-816.
14. J. Y. Lee, S. T. Connor, Y. Cui and P. Peumans, *Nano Lett.*, 2008, **8**, 689-692.
15. J. Song, J. Li, J. Xu and H. Zeng, *Nano Lett.*, 2014, **14**, 6298-6305.
16. Y. H. Kim, L. Müller-Meskamp and K. Leo, *Adv. Energy Mater.*, 2015, **5**, 1401822.
17. H. Wu, D. Kong, Z. Ruan, P. C. Hsu, S. Wang, Z. Yu, T. J. Carney, L. Hu, S. Fan and Y. Cui, *Nat. Nanotechnol.*, 2013, **8**, 421-425.
18. H. G. Im, S. H. Jung, J. Jin, D. Lee, J. Lee, D. Lee, J. Y. Lee, I. D. Kim and B. S. Bae, *ACS Nano*, 2014, **8**, 10973-10979.

19. H. G. Im, J. Jin, J. H. Ko, J. Lee, J. Y. Lee and B. S. Bae, *Nanoscale*, 2013, **6**, 711-715.
20. A. Kim, Y. Won, K. Woo, C.-H. Kim and J. Moon, *ACS Nano*, 2013, **7**, 1080-1091.
21. S. Han, S. Hong, J. Ham, J. Yeo, J. Lee, B. Kang, P. Lee, J. Kwon, S. S. Lee, M. Y. Yang and S. H. Ko, *Adv Mater*, 2014, DOI: 10.1002/adma.201400474, DOI:10.1002/adma.201400474.
22. Y. Won, A. Kim, D. Lee, W. Yang, K. Woo, S. Jeong and J. Moon, *NPG Asia Mater.*, 2014, **6**, e105.
23. H. J. Kim, S. H. Lee, J. Lee, E. S. Lee, J. H. Choi, J. H. Jung, J. Y. Jung and D. G. Choi, *Small*, 2014, **10**, 3767-3774.
24. P. Lee, J. Ham, J. Lee, S. Hong, S. Han, Y. D. Suh, S. E. Lee, J. Yeo, S. S. Lee, D. Lee and S. H. Ko, *Adv. Funct. Mater.*, 2014, **24**, 5671-5678.
25. S. Hong, H. Lee, J. Lee, J. Kwon, S. Han, Y. D. Suh, H. Cho, J. Shin, J. Yeo and S. H. Ko, *Adv. Mater.*, 2015, **27**, 4744-4751.
26. B. W. An, B. G. Hyun, S. Y. Kim, M. Kim, M. S. Lee, K. Lee, J. B. Koo, H. Y. Chu, B. S. Bae and J. U. Park, *Nano Lett.*, 2014, **14**, 6322-6328.
27. J. Jin, J. H. Ko, S. Yang and B. S. Bae, *Adv. Mater.*, 2010, **22**, 4510-4515.
28. J. H. Lee, P. Lee, D. Lee, S. S. Lee and S. H. Ko, *Cryst. Growth Des.*, 2012, **12**, 5598-5605.
29. M. Song, D. S. You, K. Lim, S. Park, S. Jung, C. S. Kim, D.-H. Kim, D.-G. Kim, J.-K. Kim, J. Park, Y.-C. Kang, J. Heo, S.-H. Jin, J. H. Park and J.-W. Kang, *Adv. Funct. Mater.*, 2013, **23**, 4177-4184.
30. C. Bao, J. Yang, F. Li, Y. Yao, B. Yang, G. Fu, X. Zhou, T. Yu, Y. Qin, J. Liu and Z. Zou, *ACS Nano*, 2015, **9**, 2502-2509.
31. B. Han, K. Pei, Y. Huang, X. Zhang, Q. Rong, Q. Lin, Y. Guo, T. Sun, C. Guo, D. Carnahan, M. Giersig, Y. Wang, J. Gao, Z. Ren and K. Kempa, *Adv. Mater.*, 2014, **26**, 873-877.
32. T. He, A. Xie, D. H. Reneker and Y. Zhu, *ACS Nano*, 2014, **8**, 4782-4789.
33. S. Ye, A. R. Rathmell, I. E. Stewart, Y. C. Ha, A. R. Wilson, Z. Chen and B. J. Wiley, *Chem. Commun.*, 2014, **50**, 2562-2564.
34. G. Haacke, *J. Appl. Phys.*, 1976, **47**, 4086.
35. J. Jin, J. Lee, S. Jeong, S. Yang, J.-H. Ko, H.-G. Im, S.-W. Baek, J.-Y. Lee and B.-S. Bae, *Energy Environ. Sci.*, 2013, **6**, 1811-1817.
36. J. Lee, P. Lee, H. Lee, D. Lee, S. S. Lee and S. H. Ko, *Nanoscale*, 2012, **4**, 6408-6414.
37. S. Hong, J. Yeo, J. Lee, H. Lee, P. Lee, S. S. Lee and S. H. Ko, *J. Nanosci. Nanotechnol.*, 2015, **15**, 2317-2323.
38. S. C. Yang, J. H. Jin, S.-Y. Kwak and B.-S. Bae, *Macromol. Res.*, 2011, **19**, 1166-1171.

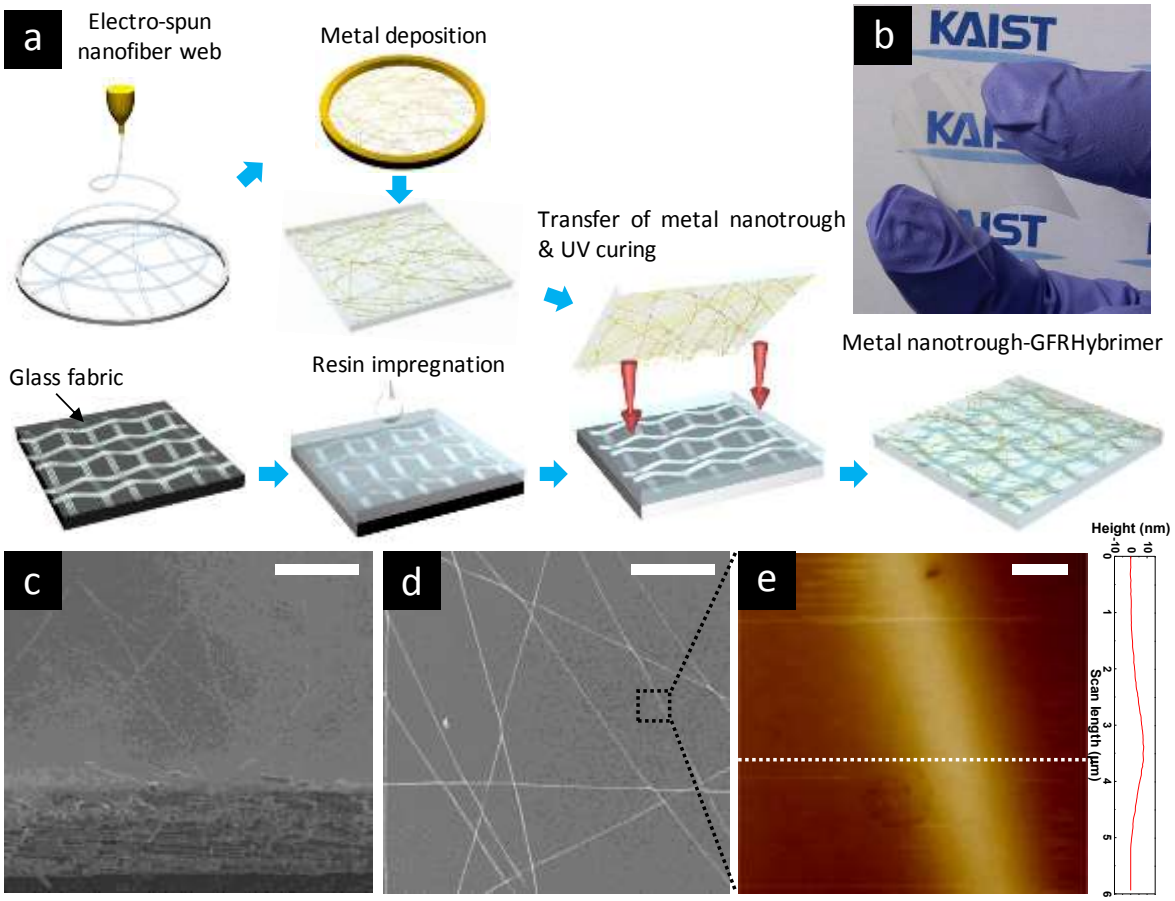

Figure 1. (a) Fabrication procedure of the metal nanotrough-GFRHybrimer film. (b) A photography of the metal nanotrough-GFRHybrimer film. (c-d) Tilted and surface SEM images of the metal nanotrough-GFRHybrimer film. The scale bars are 50 μm. (e) An AFM image of the metal nanotrough-GFRHybrimer film. The scale bar is 1 μm.

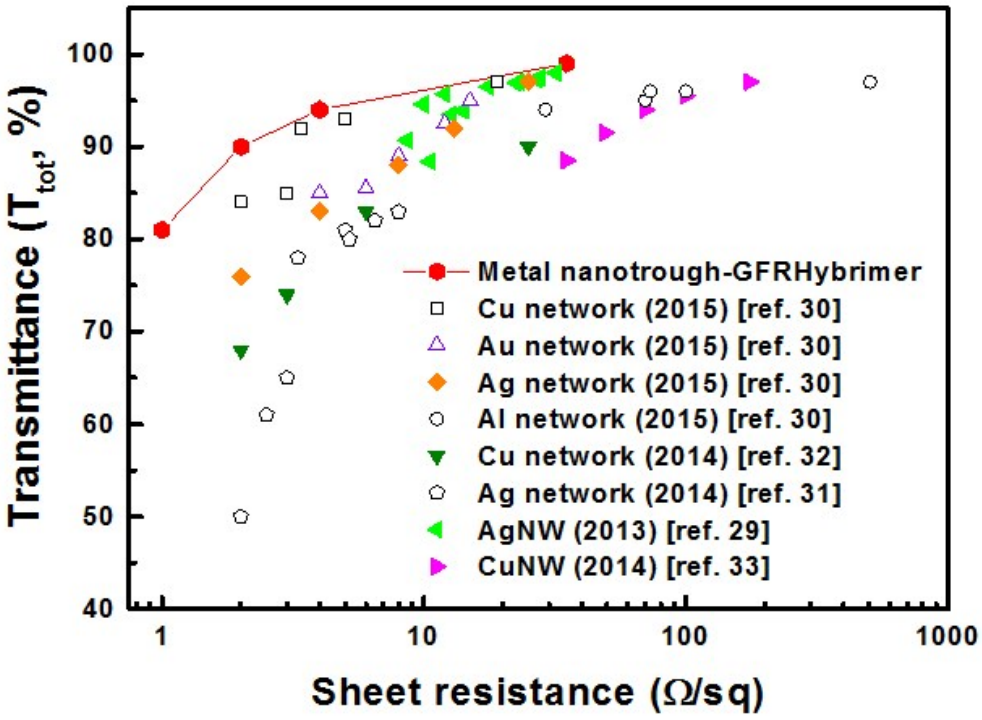

Figure 2. A plot of total transmittance at 550 nm (T_{tot}) as a function of sheet resistance (R_{sh}) for metal nanotrough-GFRHybrimer films and several recent state-of-the-art metal-based TCEs.

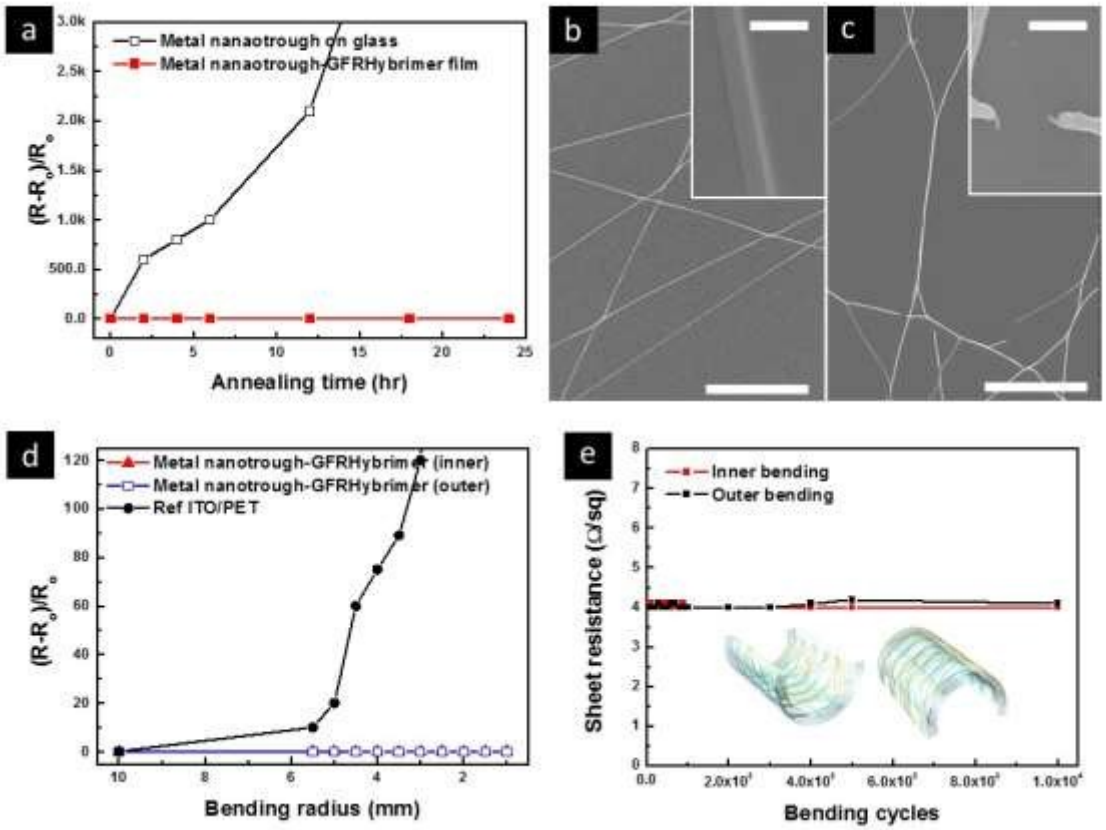

Figure 3. Thermal and mechanical stability of the metal nanotrough-GFRHybrimer film. (a) A plot of normalized sheet resistance (R_{sh}) change ($R-R_o/R_o$) versus annealing time during 250 ^oC annealing test under ambient air condition. (b-c) SEM images of the metal nanotrough-GFRHybrimer and metal nanotrough on a glass after the annealing test. The scale bars are 50 μm (The inset scale bars are 2 μm). (d) Bending test of the metal nanotrough-GFRHybrimer film with varying bending radius. (e) Repeated bending test of the metal nanotrough-GFRHybrimer film; bending radius is 1 mm.

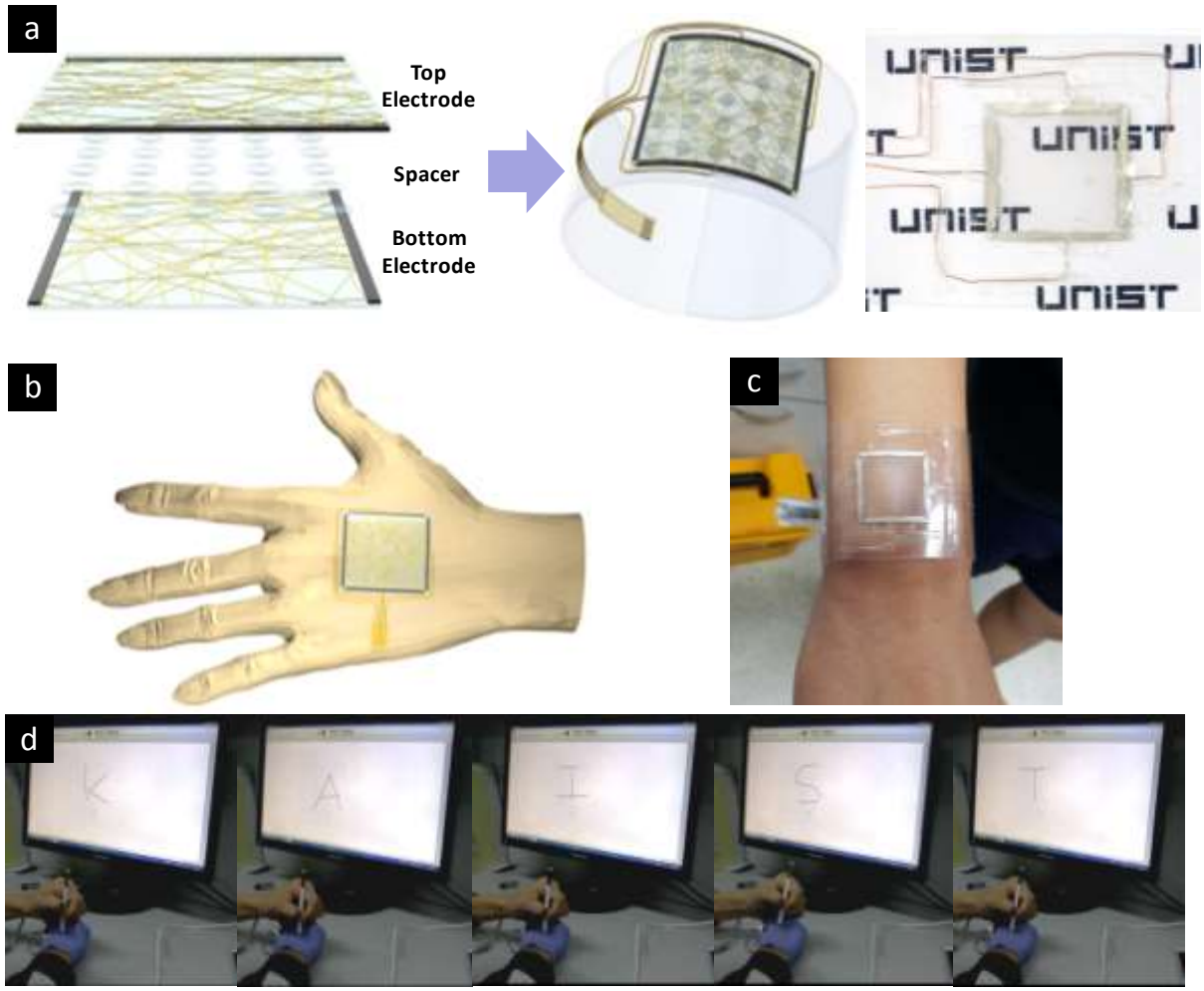

Figure 4. (a) Structure of the fabricated wearable touch screen panel using the metal nanotrough-GFRHybrimer films. (b) Schematic illustration of the integrated touch screen panel on a back of a human hand. (c) A photograph of the touch screen panel on a wristband. (d) Photographs of touch screen panel on the back of the human hand. The written characters are "KAIST".

TCE	R_{sh} (Ω sq^{-1})	*T* at 550 nm (%)	FoM (Φ_{TC}, 10^{-3} Ω^{-1})
Metal nanotrough-GFRHybrimer	**2**	**90**	**174**
C-ITO [ref. 5]	**15**	**90**	**23.2**
AgNW [ref. 35]	**15**	**94**	**24.5**
CuNW [ref. 18]	**21.2**	**90**	**16.5**

Table 1 R_{sh}, total transmittance, and corresponding figure of merit (FoM) values of the metal nanotrough-GFRHybrimer film. Reference data sets are also included.

The table of contents entry

Junction resistance-free continuous metal nanotrough-embedded transparent conducting electrode (TCE) composite film (metal nanotrough-GFRHybrimer film).